Transactions on Engineering Sciences vol 34, © 2001 WIT Press, www.witpress.com, ISSN 1743-3533

Advances in surface analysis technology

X.Q. Jiang & L. Blunt
University of Huddersfield, United Kingdom

Abstract

The needs of modern surface metrology assessment cover not only the extraction of roughness, waviness, but also identification of surface texture or the multi-scalar properties of a surface topography. In answer to this, the newly developing wavelet theory has been introduced into surface characterisation in 1994. Wavelet analysis employs time-frequency windows and offers the relevant time-frequency analysis, as a result, it can divide surface topography into different frequency components, and then study each component with the multi-resolution. This paper provides a survey of the most recent work in the field of surface metrology by using wavelet theory. The major wavelet models used in surface metrology will be introduced and the basic theory, algorithm and the properties of these models will also be discussed.

1 Introduction

Typical surface analysis only considers the extraction of roughness and waviness components of a surface. This is normally accomplished by using filtering techniques, especially Gaussian filtering [1-2]. Gaussian filtering, used for the extraction of the roughness and waviness components, is based on a presupposition: a surface signal is a combination of a series of harmonic components. If surface waveforms conform to the assumption, the roughness and waviness can be well identified and extracted from the original surfaces though with a modified amplitude resulting from the transmission characteristics of a Gaussian function [3].

Identification of topographic features of engineering surface has been made by Whitehouse and Zhang [4-5]. The energy distribution in the space-frequency plane, offered by the Wigner transform, can be used to identify the variation of surface topography. The result of this is that information about the frequencies

and their locations within a surface signal have been used to monitor and adjust the manufacturing process. However, a reasonable algorithm that allows reconstruction of atomic decomposition of a signal by using the Wigner transform does not exist [6].

Analysis of multi-scalar properties of a surface topography needs to not only provide both the frequencies of the signal and their location, but also is expected to accurately recover and perfectly reconstruct these topographic features. Considering the needs of surface assessment, wavelet analysis has been applied to surface characterisation since 1994. Many papers have shown examples in the surface metrology field. In this review, the major wavelet models used in surface metrology are considered. The basic theory, algorithm and the properties of these models are introduced and discussed.

2 Brief wavelet theory

One basic idea behind wavelet analysis is to transfer a complex frequency analysis to a simple scalar analysis. Wavelet analysis employs time-frequency windows and offers the relevant time-frequency analysis, which uses long windows at low frequencies and short windows at high frequencies (shown in Figure 1*a*). Wavelets provide a mathematical microscope that *"can divide functions into different frequency components, and then study each component with a resolution which is matched to its scale"* [7-8]. The wavelet transform is an update of the classical Short-Time Fourier Transform (STFT) or Gabor Transform [9-10] as well as the Wigner distribution. In contrast to wavelet analysis, STFT uses a single analysis window (shown in Figure 1*b*), and offers the same accurate analysis in the whole time-frequency plane. The wavelet transform is related to space-frequency analysis and is similar to the Wigner-Ville distribution [11]. A point to be noted is that Wavelet analysis takes the signal decomposition to a space-scalar (time-frequency) plane, and separates then reconstructs these components in the space domain. In contrast, Wigner analysis

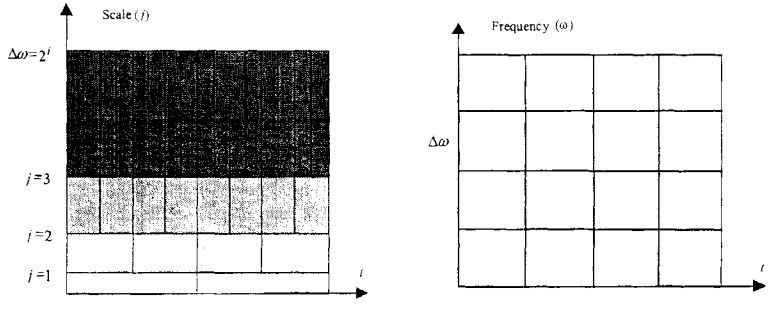

(a) Time (Space) - Scale Window *(b) Time (Space) - Frequency Window*

Figure1 the different windows of the wavelet and the STFT

also decomposes a signal into the space-frequency plane, then studies the energy distribution of these components but they can not be recovered and reconstructed perfectly.

The wavelet transform has proved to be a powerful tool for various applications. The Wavelet technique includes many different wavelet functions but each has its own properties and applications. In the field of surface metrology, continuing and discrete wavelet models have been developed.

3 Continuous wavelet

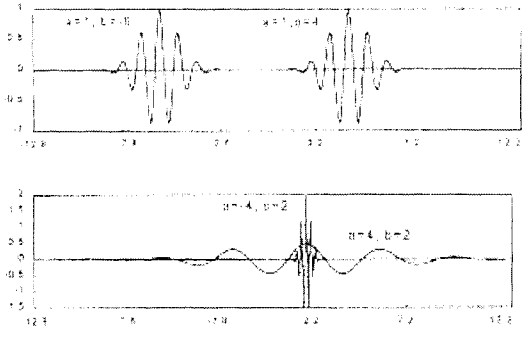

Figure 2 the dilation and translation of continuous wavelet [12]

A wavelet is a waveform that has compact support in both the space and frequency domains and whose integral is zero. In wavelet analysis the signal is broken down into rescaled and shifted versions of the original waveform. This then transfers space based information into scale based information, which represents the frequency and location properties of the original signal. In one-dimension, the wavelets, $\psi_{a,b}(t)$, (basis functions) can be obtained by dilation and translation of the prototype wavelet $\psi(t)$. a is the scalar parameter that can be used to illustrate dynamic transmission bandwidths or cover different frequency ranges, and b is the translation parameter as shown in Figure 2. Typical one-dimensional continuous wavelets are expressed by:-

$$\psi_{a,b}(x) = \frac{1}{\sqrt{a}}\psi(\frac{x-b}{a}) \tag{1}$$

In 1997, Lee and Zahouuani *et al.* [12] proposed a continuing wavelet model for visualisation of engineering surfaces. In their work, four wavelets had been initially tried. The frequency characterisation of a surface signal was analysed using the Morlet and Barrat wavelet whereas the scalar property of a signal was characterised using a nth Gaussian wavelet.

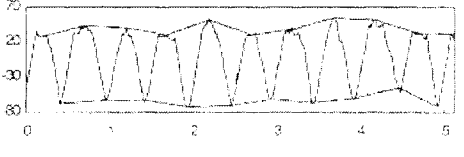

Figure 3 the result of continuous wavelet transform from a periodic surface with a 2^{nd} Gaussian derivation [12]

The continuous wavelet transform and inverse transform can then be defined as:

$$\begin{cases} W_{a,b}(x) = \dfrac{1}{\sqrt{a}} \int_{-\infty}^{\infty} f(x)\psi^*(\dfrac{x-b}{a})dx \\ f(x) = \dfrac{1}{C_g} \int_{-\infty}^{\infty}\int_{-\infty}^{\infty} \dfrac{1}{\sqrt{a}} W_{a,b}(x)\psi(\dfrac{x-b}{a})\dfrac{dadb}{da^2} \end{cases} \tag{2}$$

The authors give a simulated example, in which the singularities of a continuous profile are determined by detecting the local maximum of the modulus. Figure 3 shows the result of the wavelet transform for the periodic profile with a 2nd Gaussian derivation wavelet. The distinction between the peak or pit morphology can be obtained by using an instantaneous phase variation. The first derivation of a signal permits localisation of the pit position, that is, the maximum of the phase derivation; the peak position is detected by the derivation of the phase after a $\pi/2$ translation in the phase domain. The maximum of the derivation corresponds to the peak position. Therefore, the superior envelope (peak envelope) and inferior envelope (pit envelope) can be determined.

4 Discrete wavelet

In the real world, most signals are in discrete data sets. Hence only discrete wavelet transform is a real, practical and acceptable analysis tool. In the discrete case, the dilation and translation parameters both take only discrete values. The rescaled wavelets, $\psi_{j,0}(t) = \psi(a^{-j}t)$ are dilated by the factor a^{-j}, when $a = 2$ as shown in Figure 4*a*. j is the scalar parameter that can be used to illustrate dynamic transmission bandwidths or cover different frequency ranges. The shifted wavelets $\psi_{0,k}(t) = \psi(t-k)$ are translated by k (translation parameter) as shown in Figure 4*b*. Changing k, the time location centre has been moved. Typical one-dimensional wavelets $\psi_{j,k}(x)$ are dilated j times and shifted k times. The discrete wavelets are expressed by:-

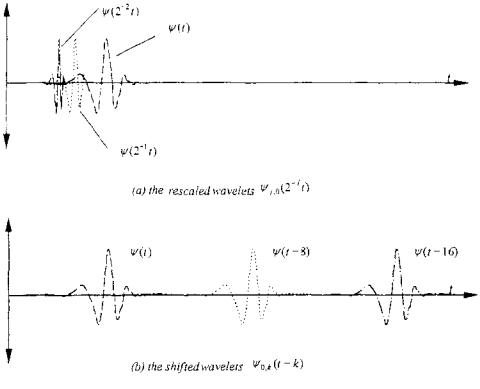

Figure 4 the discrete wavelet

$$\psi_{j,k}(x) = a^{-j/2}\psi(a^{-j}x - k) \tag{3}$$

Thus a signal is divided into different scales, with the signal data now being represented on a 'time-scalar plane'. Multi-resolution divides the frequencies into

octave bands, from ω to 2ω. Frequencies shift upward by an octave when time is rescaled by two. Figure 1*a* shows how the time-frequency plane is partitioned naturally into rectangles of constant area.

For a discrete signal $y(x) \in L^2(Z)$, its discrete wavelet transform can be expressed by:-

$$W_{j,k}(y) = \left\langle y(x), \psi_{j,k}(x) \right\rangle = 2^{-j/2} \sum_{j,k} y(x) \psi(2^{-j}x - k) \tag{4}$$

It was shown by Daubechies and Chui [7-8] that the discrete wavelet transform is reversible. So the signal $y(x)$ can be recovered with the following equation

$$y(x) = \left\langle y(x), \psi_{j,k}(x) \right\rangle \Psi_{j,k}(x) \tag{5}$$

where, the $\Psi_{j,k} = (F * F)^{-1} \psi_{j,k}$. The main approach to wavelets uses a two-channel filter bank as shown in Figure 5, and the dilation equation of the basis wavelets and corresponding scaling functions develop lowpass H_0 and highpass H_1 filter coefficients.

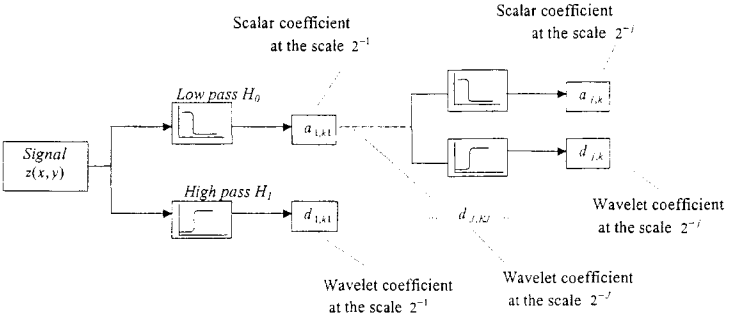

Figure 5 the decomposition of the original signal $z(x, y)$

4.1. Orthogonal wavelet

A popular wavelet is the Daubechies or so-called orthogonal wavelet. It was first used for surface analysis by Chen & Raja *et al.* and Jiang & Li [13-14]. The orthogonal wavelet has a finite impulse, compact support and can be reconstructed perfectly. Figure 6 gives the transmission characteristics of the lowpass filter bank created by a Daubechies wavelet

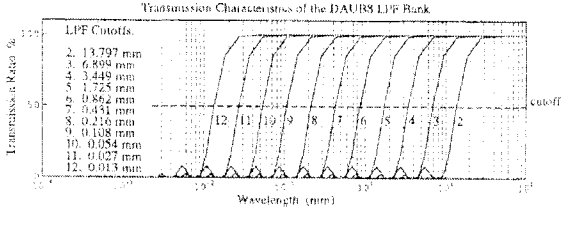

Figure 6 transmission characteristics of the multi-channel low filter bank using orthogonal wavelet with order 8 [13]

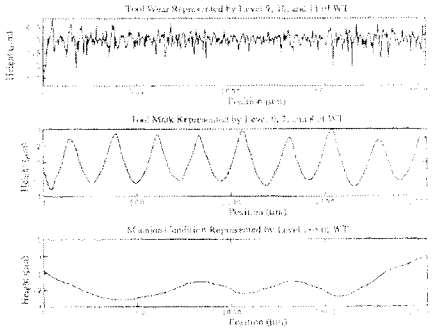

Figure 7 the separation of the surface profile based on cause in manufacturing [13]

with order 8. Using this wavelet property, the examination of the features of the signal present over the whole recorded time period was allowed. Chen & Raja *et al.* analysed a turning process and the rough profile as shown in Figure 7. The wavelet detail levels up to level 5 constitute the region indicating the machine condition; wavelet details in level 6,7, and 8 together make up the basic tool mark of turning process; and level 9 and above give the irregular components caused by tool wear.

However, the main problem with the orthogonal wavelet is that the approach itself generates wavelets. In the orthogonal case, the wavelet uses a two-channel filter bank, and the dilation equations of the basis wavelets and corresponding scaling functions develop lowpass H_0 and highpass H_1 filter coefficients. However, due to the fact that the frequency responses of the two-channel filters, so-called analysing filters, are not ideal brick wall filters, this normally lead to aliasing, amplitude modification and phase distortion. As a consequence, a normally orthogonal wavelet with a high order was used to improve the phenomenon resulting from phase distortion.

4.2. First generation biorthogonal wavelet

The requirement for filtering surface data includes: linear phase shift, finite pulse response and perfect reconstruction, only biorthogonal wavelet satisfies these conditions. In order to overcome these defects, the biorthogonal wavelet for surface analysis has been proposed by Jiang & Blunt *et al.* in 1997 [15].

The biorthogonal wavelet allows the construction of a symmetric wavelet and thus a linear phase filter. In the biorthogonal case, the other two-channel filters: G_0 and G_1 (so-called synthesis filters), have been specially designed to compensate for these errors of the analysing filters H_0 and H_1. When the frequency responses of the synthesis filters, $G_0(z)$, $G_1(z)$, are the inverses of the analysis filters, $H_0(z)$, $H_1(z)$ and they satisfy [19]

$$\begin{aligned} G_0(z)H_0(z) + G_1(z)H_1(z) &= 2z^{-l} \\ G_0(z)H_0(-z) + G_1(z)H_1(-z) &= 0 \end{aligned} \tag{6}$$

the errors in this analysis bank are cancelled. Where, l is time delay, the distortion term must be z^{-l}, and aliasing term must be zero. This means that the two-channel filter banks should be biorthogonal. In the biorthogonal case, the impulse responses, $h_0(k)$, $h_1(k)$, of analysis filters would not be double-shift orthogonal to themselves, but they would be double-shift biorthogonal to $g_0(k)$, $g_1(k)$, of the synthesis filters.

In that case, the wavelet details are computed by separate filtering of the signal $z(x, y)$ along the abscissa and ordinate. The wavelet decomposition can thus be interpreted as a signal decomposition in a set of independent, spatially oriented frequency channels.

An interesting example is shown in Figure 8. Figure 8*a* presents the 3D concave bearing surface of the equatorial region of a precision polished acetabular cup used in hip replacement. It was obtained by scanning the surface topography using a stylus instrument, which employs an x-gearbox and a y-translation table with a precision lead screw for translation of the specimen. The figure clearly shows that the surface topographies of the measured acetabular cup include a very considerable amount of table error derived from the y-axis of the measurement instrument. As shown in Figure 8*b*, the y-axis table error, which influences the horizontal high frequencies of roughness, have been separated. In comparison with figure 8*a*, the multiscalar features have been reconstructed accurately and the localised positions of the peaks or pits/scratches have been retained precisely in Figure 8*b*. The table error caused by the 3D stylus measurement has clearly been "filtered out".

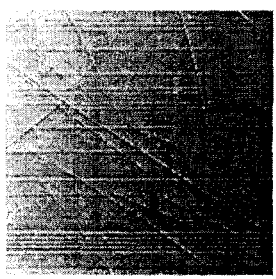

(a) the raw measurement data head

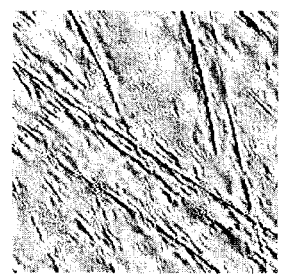

(b) the filtered data

Figure 8 the measured map and multiscalar map of the bearing surface of a precision acetabular cup

The significant point of the biorthogonal wavelet is that it has *a brick wall, linear phase* (leading to real output without aliasing and phase distortion) *and a traceably located property* so that the different component surfaces obtained are a more natural record of the real surface. However due to the fact that wavelets, $\psi_{j,k}(t)$, (basic functions) are built by dilation and translation of the prototype wavelet $\psi(t)$ which relied on the Fourier transform. The wavelet transform needs to be applied along three directions, horizontal, vertical, and

diagonal [7, 16]. The theory and corresponding algorithm [7-8, 15-18] are very complex, and a great deal of computer memory and computation time is needed. Furthermore, there is still the boundary data destruction inherent when using the Fourier transform.

4.3 Second generation biorthogonal wavelet

For industrial application purposes the method used for surface functional characterisation should have considerable merits. It needs to be simple and natural. In other words, the method of separation and reconstruction of different components of the surface should have both the 'simplicity' of a Gaussian filter and 'naturalness' of a biorthognal wavelet filter. From the point of view of the above requirement, a lifting wavelet model (based on the algorithm of a second generation wavelet [19-20]) has been developed by Jiang & Blunt, and Scott [21-22].

The second generation algorithm uses the lifting scheme to replace the Fourier transform as its construction tool and gives up the dilation and translation, but it still preserves all properties of the first generation algorithm. In this implementation, the analysis highpass filter, H_1, and synthesis lowpass filter, G_0, of the initial finite biorthogonal wavelet filter set, $\{H_0, H_1, G_0, G_1\}$ within the first generation are transferred to $H_1^{'}$, $G_0^{'}$ which can be found by the lifting scheme as

$$\begin{cases} H_1^{'}(z) = H_1(z) + G_1(z)S(z^2) \\ G_0^{'}(z) = G_0(z) - H_0(z)S(z^{-2}) \end{cases} \tag{7}$$

where the $S(z)$ is a Laurent polynomial.

Following the above idea, the algorithm of the forward lifting wavelet transform can be described by:-

$$\begin{cases} A_{j,2k}, A_{j,2k+1} = Split(A_j) \\ d_{j+1,k} = A_{j,2k+1} - \rho(A_{j,2k}) \\ a_{j+1,k} = A_{j,2k} + \mu(d_{j+1,k}) \end{cases} \tag{8}$$

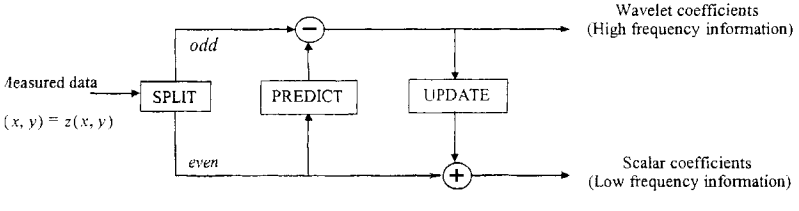

Figure 9 the lifting scheme

The above illustrates significant built-in features that predict, ρ, and update, μ, can be flexibly designed by the coefficient $s(\cdot)$ and the Laurent polynomial

$S(z)$ according to the intending requirement of surface analysis. The block diagram of the two lifting steps is given in Figure 9.

Using an inverse wavelet transform, high and low frequencies can be recovered flexibly and immediately in the different transmission bands in terms of the functional analysis requirements. The inverse wavelet transform is simply performed by reversing the operation and toggling negative to positive for all operations.

Figure 10*a* shows the precision lapped topography in the polar region of a new ceramic replacement femoral head with sampling area $300 \times 240 \mu m$. The surfaces look 'fine and smooth' and have isolated large pits. Figure 10*b* shows how the wavelet model has removed roughness, waviness and form deviation revealing the functionally significant multiscalar feature surfaces.

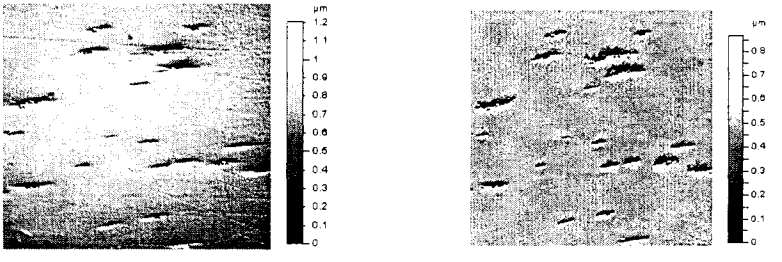

(a) a raw measured surface *(b) a morphological surface*

Figure 10 The measured and morphological surfaces of a worn ceramic head

Figure 11*a* shows slope intensity image of the measured data of a worn metallic femoral head surface. The functional surface, derived from the wavelet filtering method, is shown in the figure 11*b*. It can be seen that the two images are similar to each other without any relative phase shift in sampling area. The peak-valley information on the bearing surfaces is also recorded completely.

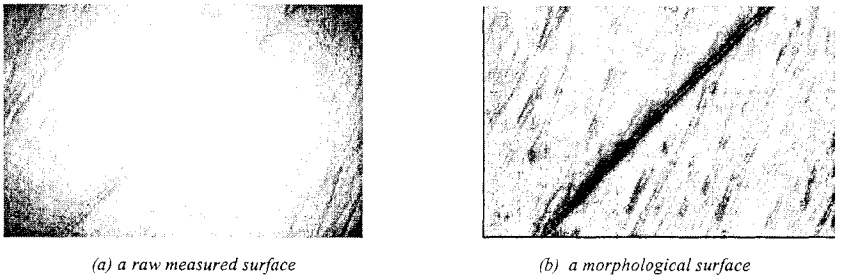

(a) a raw measured surface *(b) a morphological surface*

Figure 11 The measured and morphological surfaces of a worn ceramic head

It is quite possible that classical problems of extraction of different surface waves can also be solved using this simple wavelet filter algorithm. The wavelet technique provides a potential tool that has been shown to be very successful for surface metrology.

References

1. Whitehouse, D.J., *Surface Metrology*, 1st edn, Bristol and Philadephia, Institute of physics publishing, 1994.
2. Stout, K.J., Sullivan, P.J., Dong, W.P., Mainsah, E., Luo, N., Mathia, T. & Zahyouani H., *The development of methods for the characterisation of roughness in three dimensions,* 1st edn, Commission of the European Communities (ISBN 0 70441 313 2), 1993.
3. ISO 11562: *Surface texture – Metrological characterisation of phase correct filters*, (International Standard Organization, Geneva), 1994.
4. Whitehouse, D.J. and Zhang, K.G., The use of dual space-frequency functions in machine tool monitoring, *Meas. Sci. Technol.*, 3, pp.796-808, 1992.
5. Zhang, K. and Whitehouse, D.J., The application of the Wigner distribution function to machine tool monitoring, . *Proc., Inst. Mech. Eng*, 206, pp. 249-264, 1992.
6. Meyer, Y., *Wavelets: algorithms and applications*, 1st edn, Philadelphia, SIAM, 1993.
7. Daubechies, I., *Ten lectures on Wavelets*, 1st edn, Philadelphia, SIAM, 1992.
8. Chui, C.K. *An Introduction on Wavelets*, Philadelphia, SIAM, 1992.
9. Gabor, D. Theory of communication, *J. of the IEE*, 93, pp.429-457, 1946.
10. Allen, J. B. and Rabiner, L. R. Aunified approach Short-Time Fourier analysis and synthesis, *Proc. IEEE*, 65, pp.1558-1564, 1977.
11. Wigner, E., On the quantum correction for thermo dynamic equilibrium, *Phys. Rev.*, 40, pp.749-759, 1932.
12. Lee, S-H., Zahouani, H., Caterini, R. and Mathia, T.G., Multi-scale analysis of engineering surfaces. *Int. J. Mach. Tools Manufact.*, 38, pp.581-589, 1998.
13. Chen, X., Raja, J. and Simanapalli, S., Multi-scale analysis of engineering surfaces. *Int. J. Mach. Tools Manufact.*, 35, pp.231-238, 1995.
14. Jiang, X.Q. and Li Z., *The development Wavelet spectral analysis system for surface characterisation*, NNSF No: 59375255, China, 1994.
15. Jiang, X.Q., Blunt, L. & Stout, K.J., Three-dimensional surface characterisation for orthopaedic joint prostheses. *Proc., Inst. Mech. Eng.*, 213, pp.49-68, 1999.
16. Strang, G. & Nguyen, T., *Wavelets and filter banks*, 1st edn, Wellesley-Cambridge Press, 1996.
17. Mallat, S.Q., A theory for multiresolution signal decomposition: The Wavelet representation, *IEEE transaction on pattern analysis and machine* intelligence, 11, pp. 674-693, 1989.
18. Daubechies, I., The Wavelet transform time-frequency localisation and signal analysis. IEEE Trans. on Info. Theory, 36, pp.961-1005, 1990.
19. Swelden, W., The lifting scheme: a custom-design construction of biorthogonal Wavelets, Bell Laboratories, 1995.

20. Swelden, W. The lifting scheme: a construction of second generation Wavelets, Bell Laboratories, 1996.
21. X.Q. Jiang, L. Blunt and K.J. Stout, Development of a lifting wavelet representation for surface characterisation, *Proc. R. Soc. Lond. A*, 456, 1-31, 2001.
22. ISO/TS 16610-4, Data extraction techniques by sampling and filtration Part 4 – Spline Wavelets (Under preparation), 1999.